Spontaneous Article

Silicification of feathers in a modern hot spring in New Zealand

Tao ZHAO[1]*, Liang HU[2,3] and Yanhong PAN[1]

[1] State Key Laboratory for Mineral Deposits Research, School of Earth Sciences and Engineering, Centre for Research and Education on Biological Evolution and Environment, Frontiers Science Center for Critical Earth Material Cycling, Nanjing University, Nanjing 210023, China.
[2] State Key Laboratory of Palaeobiology and Stratigraphy, Nanjing Institute of Geology and Palaeontology and Center for Excellence in Life and Paleoenvironment, Chinese Academy of Sciences, Nanjing 210008, China.
[3] University of Chinese Academy of Sciences, Beijing 100049, China.
*Corresponding author. Email: zhaotao@nju.edu.cn

ABSTRACT: Fossil feathers have greatly improved our understanding of the evolutionary transition from non-avian dinosaurs to birds and the evolution of feathers, and may be the only evidence for their source animals in the fossil record. Hot spring environments have been demonstrated to be conducive to the preservation of fossils, but internal silicification of feathers was not observed in the only avian carcass so far discovered in ancient hot spring deposits. To determine whether feathers can be internally silicified, here we analyse feathers sampled from a modern hot spring vent pool – Champagne Pool – in New Zealand. Our results of scanning electron microscopy (SEM)-energy dispersive X-ray spectrometry elemental mapping show that the sampled feathers are silicified to different degrees, and one of them is pervasively silicified. SEM observations show that feathers can be silicified at the cellular level. Degradation is involved in the silicification of feathers, as indicated by the reduction of the abundance of carbon and the loss of keratin fibrils. Our findings suggest that ancient deposits of hot spring vent pools are promising targets in search for fossil feathers.

KEY WORDS: birds, exceptional preservation, fossil feathers, opal-A fabrics, taphonomy.

Feathers are unique to birds among extant vertebrates. The major structural proteins of feathers, β-keratins (also referred to as corneous beta-proteins) (Alibardi 2013, 2017), are resistant to degradation, which is considered to be a reason why feathers are relatively common in the fossil record (Davis & Briggs 1995; Schweitzer 2011; Kamarudin *et al*. 2017; Schweitzer *et al*. 2018; Benton *et al*. 2019). Discoveries of feathers in non-avian dinosaurs indicate that feathers originated long before birds (Ji & Ji 1996; Xu & Guo 2009; Xu *et al*. 2014; Benton *et al*. 2019). Fossil feathers have played an important role in our understanding of evolution of feathers and flight (Longrich *et al*. 2012; Zheng *et al*. 2013; Foth *et al*. 2014; Xu *et al*. 2014; Feo *et al*. 2015; Benton *et al*. 2019; Pan *et al*. 2019). Often, fossil feathers are the only evidence for their source animals (Davis & Briggs 1995; Xing *et al*. 2020). To date, reported fossil feathers are mainly preserved as compressions (e.g., Davis & Briggs 1995; Zhang *et al*. 2006; Xu & Guo 2009), impressions (Longrich *et al*. 2012; Foth *et al*. 2014), or in amber (e.g., Perrichot *et al*. 2008; McKellar *et al*. 2011; Xing *et al*. 2020). Less common are feathers preserved in coprolites (Wetmore 1943) and in hot spring deposits (Channing *et al*. 2005).

Ancient siliceous hot spring deposits (sinters) have been demonstrated to be highly productive for the recovery of exceptionally preserved fossils, which may even include cellular details (e.g., Channing & Edwards 2013; Massini *et al*. 2016; Dunlop & Garwood 2018; Garwood *et al*. 2020). For example, the preservation of the cellular details of the lycopsid *Asteroxylon mackiei* from the Devonian Rhynie chert allows the identification of the oldest meristems of rooting axes (Hetherington & Dolan 2018). However, internal silicification of feathers and fine details at the cellular level were not observed in the only avian carcass so far discovered in ancient siliceous hot spring deposits of Yellowstone National Park (Channing *et al*. 2005).

Though there is only one report of feathers from ancient hot spring deposits (Channing *et al*. 2005), feathers are found to be common in modern hot springs (Jones & Renaut 2003). To determine whether feathers can be internally silicified, here we analyse feathers sampled from a modern hot spring – Champagne Pool – in the Waiotapu geothermal area, Taupo Volcanic Zone, New Zealand. Our results have implications for understanding the preservation potential of feathers in ancient hot spring deposits.

1. Material and methods

1.1. Material

Feathers preserved separately or in association with plants (Fig. 1, referred to as samples 1–3) were collected from the margin of Champagne Pool in 2018. The pool water is slightly acidic (pH 4.9–5.68) with a temperature of about 75 °C (Mountain *et al*. 2003; Pope *et al*. 2004; Pope & Brown 2014). The water contains 362–430 mg kg^{-1} silicon dioxide, which is over-saturated

 doi:10.1017/S1755691022000068

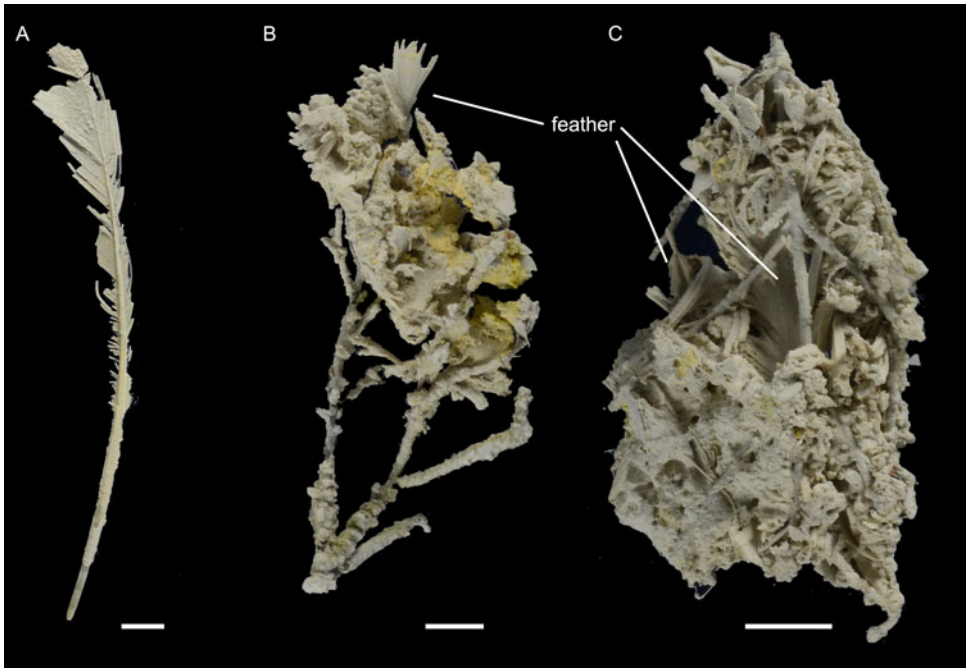

Figure 1 Photos of sampled feathers from a modern hot spring – Champagne Pool – in Waiotapu, New Zealand. (A) Sample 1. (B) Sample 2. (C) Sample 3. Scale bars = 1 cm.

with respect to amorphous silica (Mountain *et al*. 2003; Pope *et al*. 2004).

1.2. Methods

Observations and elemental analysis were performed using a Tescan MAIA3 field emission scanning electron microscope (SEM) equipped with energy dispersive X-ray spectrometry (EDS). To determine the mineralisation condition of these samples, elemental mapping was performed on two thin sections (sample 1 and sample 2) and a fracture surface (sample 3) using the SEM-EDS. Samples were coated with platinum before SEM observations and analysis.

1.3. Structure of feathers

Feathers comprise hierarchical branches of rachis, barbs, and barbules (Fig. 2a, b). The barbs consist of a cortex and a central medulla (Fig. 2c). The barb cortex is laminated and composed of keratin fibrils (Fig. 2c–e). The medulla is composed of vacuolated medullary cells (Fig. 2c, e) with fibrous membranes (Fig. 2e). In the cytoplasmic voids of the medullary cells, there are some fibrils that bridge the membranes (Fig. 2e) (Kulp *et al*. 2018).

2. Results

2.1. Elemental mapping

SEM-EDS elemental mapping shows that the feathers in the three analysed samples are silicified to different degrees (Fig. 3). The feather in sample 3 has the highest degree of silicification; silicon (Fig. 3k, o) and oxygen (Fig. 3l, p) are widespread in the barb cortex, the membranes of the medullary cells, and the barbules. Carbon is still present in the feather in sample 3 (Fig. 3j, n). As for the feathers in sample 1 and sample 2, the abundance of silicon is higher in the barbules, the membrane of medullary cells, and the outer part of the barb cortex (arrows in Fig. 3c, g) than in the inner part of the barb cortex. The abundance of carbon is lower in barbules than in the barb cortex in sample 1 (Fig. 3b). In sample 2, the abundance of carbon is lower in the barbules and the outer part of the barb cortex than in the inner part of the barb cortex (Fig. 3f). Silica is present in the medulla in all three samples (Fig. 3c, g, k).

2.2. SEM observations

The surfaces of the opal-A materials that coat the feathers are porous, containing large numbers of microorganisms, including fungi and rod-shaped bacteria (Fig. 4a, b) (see Jones *et al.* 1999a, b, 2001, 2003 for more information about microorganisms in the hot springs in the Waiotapu geothermal area). The opal-A materials below the surfaces are denser; they are granular or nonporous (Fig. 4c–e). Microorganisms are visible in nonporous opal-A on the fracture surface of sample 3 (Fig. 4e), but difficult to identify in the thin sections of samples 1 and 2 (Fig. 4c, d).

The gaps between the feathers and the surrounding sinters indicate that these feathers shrank after being encrusted by opal-A (Fig. 5a, c, e). Fracture of the outer part of the barb cortex was involved during the shrinkage (Fig. 5d, e). Fibrils of the barbules and barb cortex are evident in sample 1 (Fig. 5a). Silica particles are present within the open spaces of the barb cortex of the feather in sample 1 (arrow in Fig. 5b). Fibrils are visible in the outer part of barb cortex of the feather in sample 2 (Fig. 5d), where the abundance of silicon is high (Fig. 3g). The cytoplasmic voids of the medullary cells in sample 2 are filled with silica aggregates (Fig. 5c), while those in sample 1 (Fig. 5a) and sample 3 are not (Fig. 5e). The barb cortex of the feather in sample 3 has degraded to become hollow (arrow in Fig. 5e). The widespread distribution of silica particles in the cross section of the barb cortex also indicates the degradation of fibrils that make up the barb cortex (Fig. 5f). The membranes of the vacuolated medullary cells and the fibrils within the cytoplasmic voids in sample 3 are densely covered by silica particles (Fig. 5g).

3. Discussion

3.1. Silicification of feathers

The widespread distribution of silicon and oxygen in the cross section of the barb in sample 3 indicates that feathers can be silicified internally as well as externally. This is the first report of internal silicification of feathers, Channing *et al*. (2005) having

https://doi.org/10.1017/S1755691022000068 Published online by Cambridge University Press

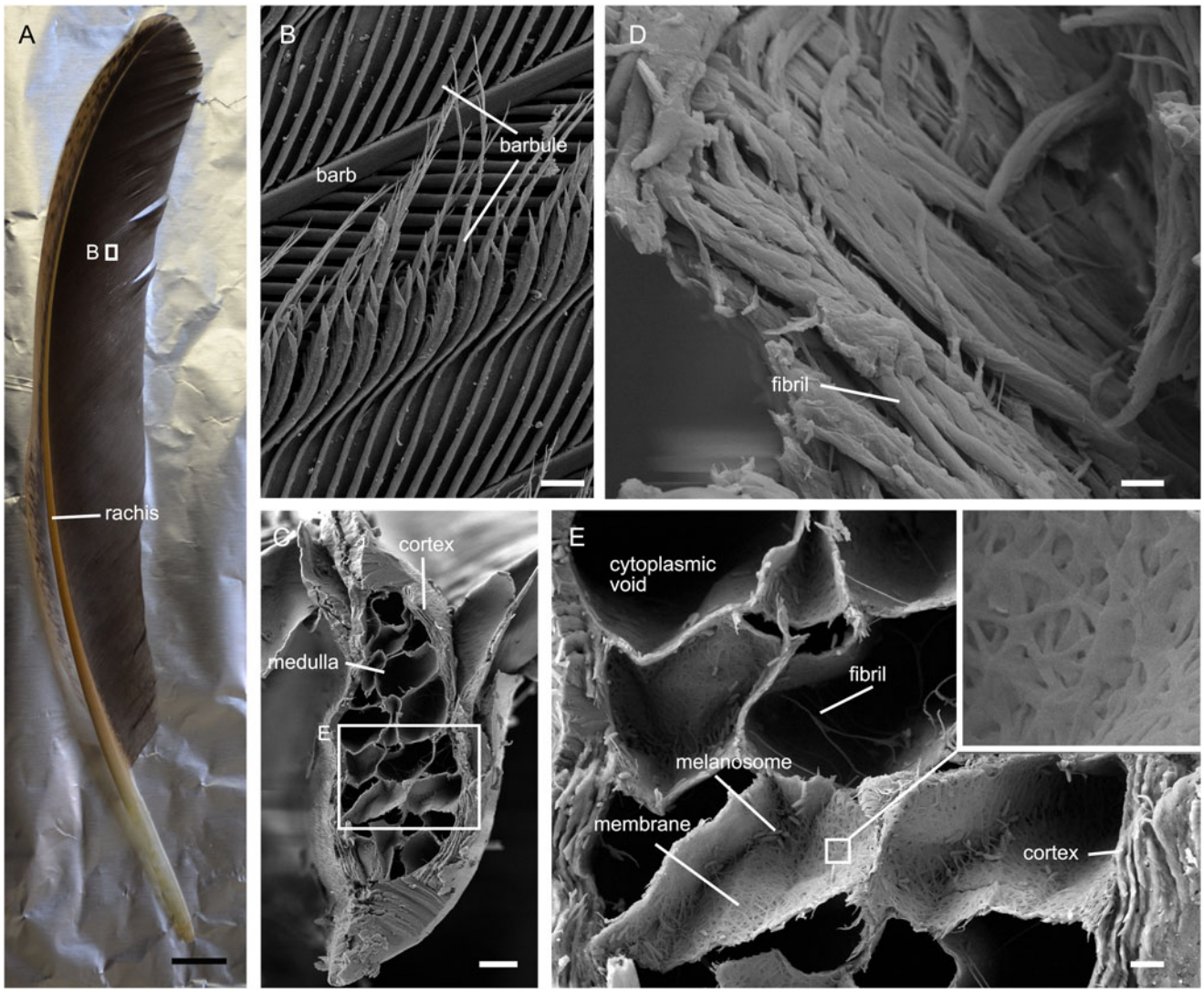

Figure 2 Photo and SEM image of chicken feathers. (A) Photo of a chicken feather. (B) Barb and barbules. (C) Cross section of a barb shows the cortex and medulla. (D) Fractured barb shows the fibrils that make up the barb cortex. (E) Cross section of a barb shows details of the medullary cells, and the laminated barb cortex. Inset in (E) shows the fibrous membrane of a medullary cell. Scale bars = 1 cm (A); 40 μm (B); 10 μm (C); 1 μm (D); 2 μm (E).

reported only encrustation of external feather surfaces. The incipient degree of silicification of the silica-encrusted feather in sample 1 suggests that the internal silicification of feathers mainly occurs after being encrusted by opal-A (Fig. 6a). The silica in the medulla (Fig. 3) indicates that silica-bearing fluids can enter the medulla and silicify feathers from the inside outwards as well as from the outside inwards (Fig. 6a). The opal-A surrounding feathers when originally formed is likely to be granular and porous, as suggested by the newly formed opal-A on the sample surfaces (Fig. 4a, b, e). Therefore, silica-rich fluids supply the silica that internally silicify the encrusted feathers by permeating through earlier formed opal-A. Along with the silicification of feathers, silica will also precipitate in pores of earlier formed opal-A, progressively reducing the porosity (Fig. 6a; Cady & Farmer 1996; Jones & Renaut 2003; Orange *et al.* 2013), which will reduce the permeation of silica-bearing fluids and may leave some empty spaces within feathers unoccupied by silica (Fig. 6a), as seen in sample 3 (Fig. 5e, f). These various features are well documented in the silicification of plants in hot spring waters (e.g., Channing & Edwards 2004, 2009).

Elemental mapping (Fig. 3) and SEM observations (Fig. 5) indicate that degradation is involved in the silicification of feathers. The abundance of carbon decreased in the barbules in sample 1, and the barbules and the outer part of the barb cortex in sample 2 (Fig. 3). The barb cortex became hollow in sample 3 because of the loss of the keratin fibrils that make up the barb cortex (Fig. 5). Degradation can create empty spaces where silica can be deposited, and facilitate the permeation of silica-supersaturated fluids (Channing & Edwards 2004). The presence of carbon in the highly silicified feather in sample 3 suggests that silicification may not necessarily lead to the total replacement of the original organic material by silica. The slight degradation of the feather in sample 1 indicates that degradation mainly occurs after being encrusted by opal-A. Though the hot spring water contains abundant microorganisms, the microorganisms near the feathers were silicified during the formation of the external opal-A encrustation. The dense opal-A encrustation can protect the feathers from decomposition by microorganisms, as well as reduce the permeation of silica-bearing fluids. It is thus likely that the degradation of feathers mainly resulted from hydrolysis. Taphonomic experiments show that entombment within silica can limit the molecular degradation of microorganisms (Toporski *et al.* 2002; Alleon *et al.* 2016), which may also apply to feathers.

The mouldic preservation of the feathers reported from the Yellowstone hot spring deposits (Channing *et al.* 2005) suggests that during degradation of these feathers, a steady supply of silica

https://doi.org/10.1017/S1755691022000068 Published online by Cambridge University Press

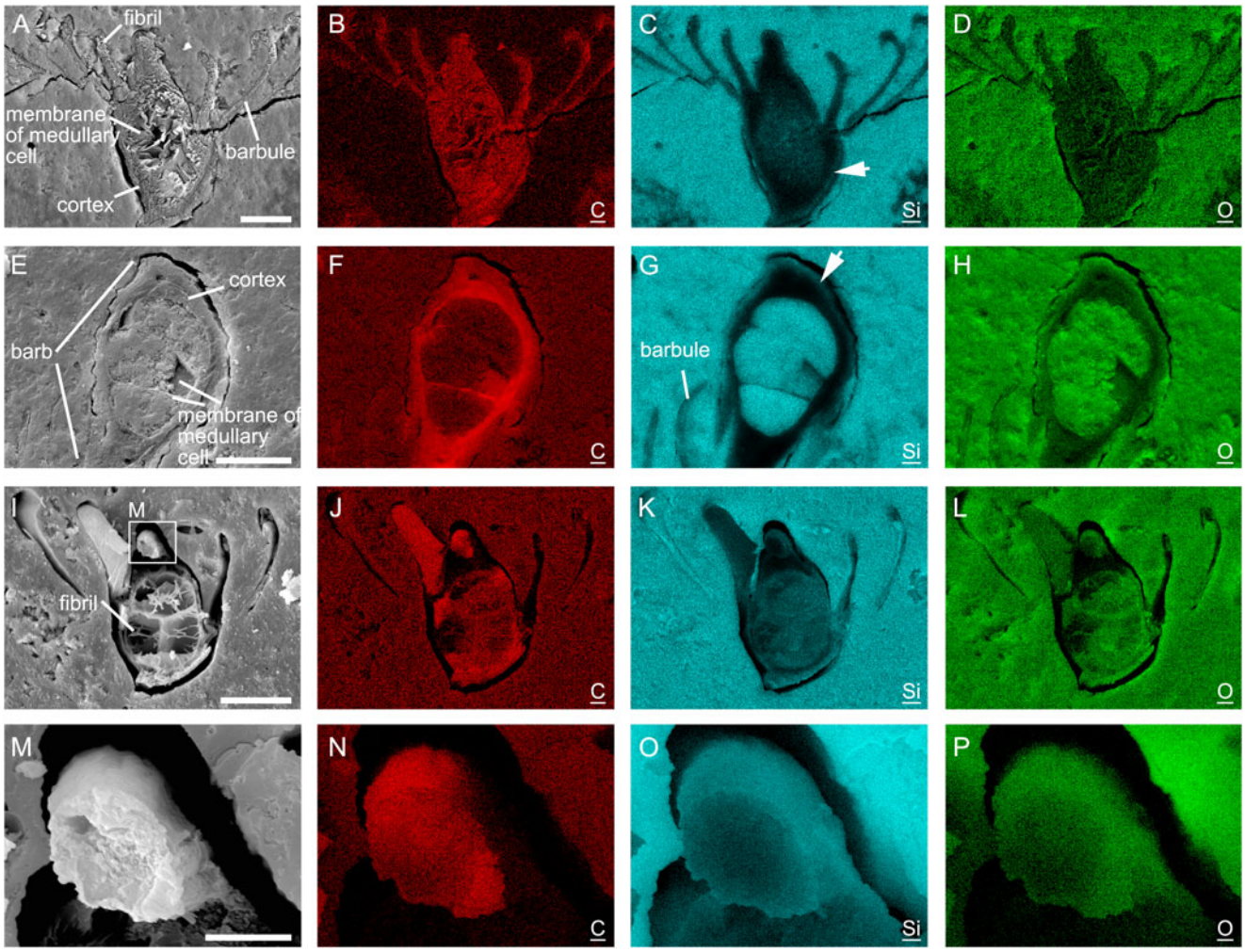

Figure 3 SEM-EDS elemental mapping of samples 1 (A–D), 2 (E–H), and 3 (I–P). Arrows in (C) and (G) point to outer part of the barb cortex where the abundance of silicon is high. C, Si, and O refer to carbon, silicon, and oxygen, respectively. Scale bars = 25 μm (A, E, I); 5 μm (M).

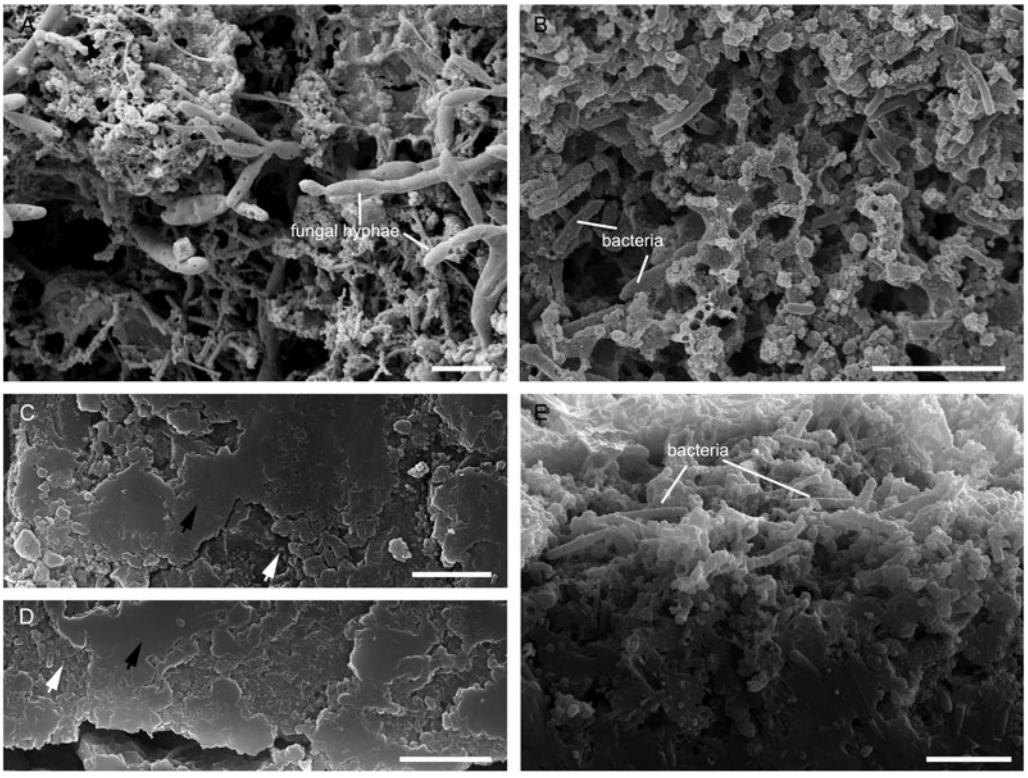

Figure 4 Opal-A fabrics of samples 1–3. (A) Surface of opal-A in sample 1. (B) Surface of opal-A in sample 3. (C) Opal-A close to feather in sample 1. (D) Opal-A close to feather in sample 2. (E) Rim of the fracture surface of opal-A in sample 3 shows the transition of the opal-A fabrics from porous to nonporous. White arrows represent granular opal-A, while black arrows represent nonporous opal-A. Scale bars = 5 μm (A, B, E); 2 μm (C, D).

https://doi.org/10.1017/S1755691022000068 Published online by Cambridge University Press

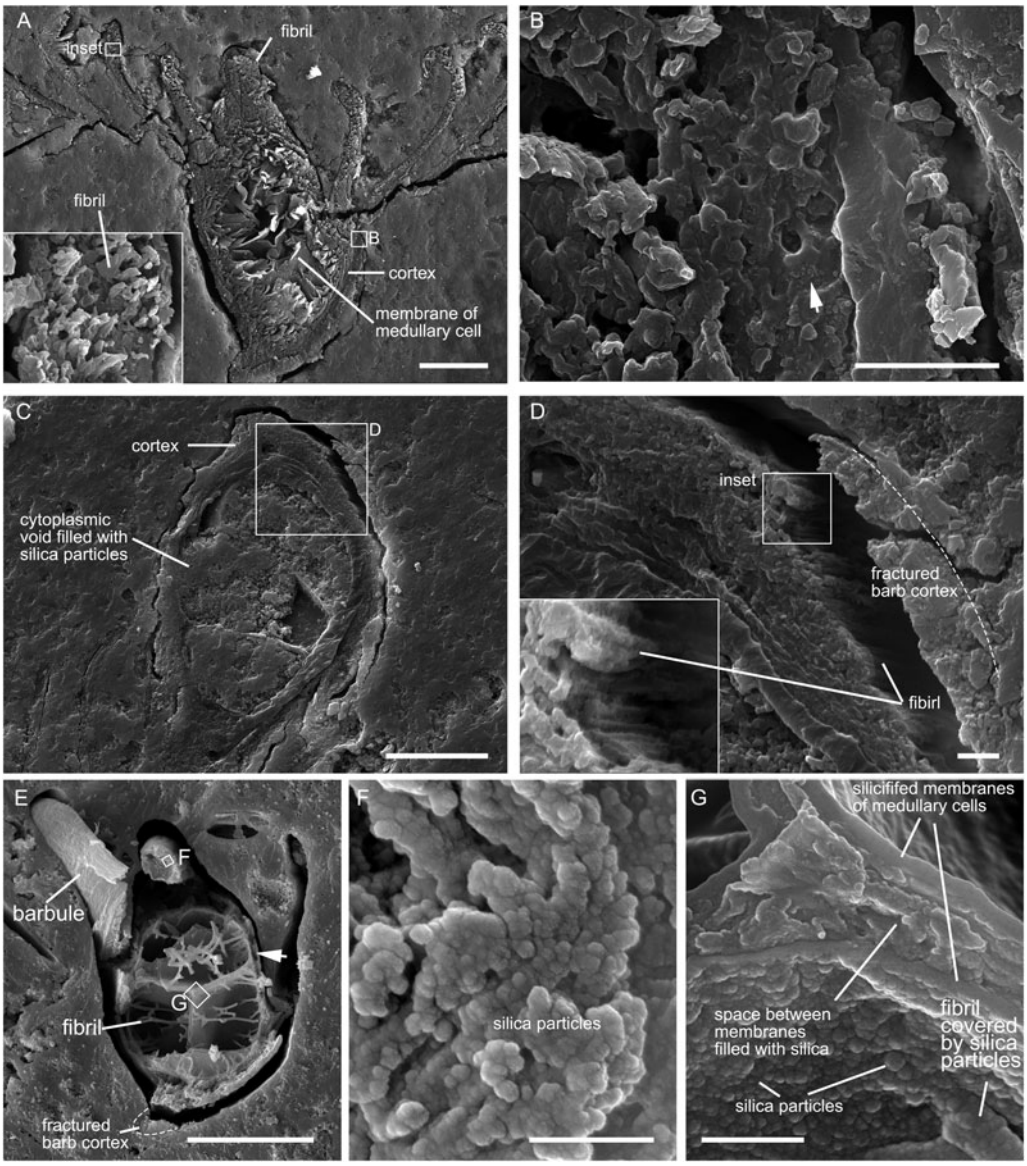

Figure 5 Morphological details of the feathers in samples 1 (A, B), 2 (C, D), and 3 (E–G). (A) Cross section of a barb and barbules shows the retention of fibrils in sample 1. Inset in (A) shows the fibrils that make up the barbule. (B) Cross section of the barb cortex in sample 1 shows the deposition of silica particles (arrow) within the open spaces within the barb cortex. (C) Cross section of a barb in sample 2 shows that the cytoplasmic voids of medullary cells are filled with silica particles. (D) Fractured part of the barb in (C) shows the retention of fibrils. (E) Fracture surface of a barb and barbules in sample 3. (F) Close-up of the barb cortex shows that silica particles largely replace the fibrils. (G) Silicified membranes of the medullary cells in sample 3. Scale bars = 20 μm (A, C); 2 μm (B, D); 25 μm (E); 500 nm (F); 1 μm (G).

was lacking – hence, these feathers were not internally silicified though being encrusted by silica deposits (Fig. 6b). The preservation of the gross morphology of a coot (*Fulica americana*) indicates that the rate of silica precipitation was high, and this aquatic bird is preserved in a hot spring vent pool or an associated high-temperature sinter terrace pool (Channing *et al.* 2005). Similarly, the feathers studied in the present study are also from a hot spring vent pool – Champagne Pool – in New Zealand (Campbell *et al.* 2015). However, a key difference between the feathers from the Yellowstone hot spring deposits and the feathers in the present study is that the feathers from the Yellowstone hot spring deposits were attached to a carcass, while the feathers in the present study are isolated. The plumage of many aquatic birds is specialised to avoid wetting the skin and losing heat during swimming and diving (Yang *et al.* 2006). It is likely that the opal-A encrustation surrounding the whole bird and the arrangement of the feathers limited the permeation of silica-bearing fluids, which resulted in the mouldic preservation.

3.2. Implications for exploration of silicified feathers in ancient siliceous hot spring deposits

As feathers are a common component of the biodebris in modern hot springs (Jones & Renaut 2003), silicified feathers are unlikely to be rare in the Jurassic and post-Jurassic hot spring deposits. The fossil record shows that feathers appeared in the Jurassic (Foth *et al.* 2014; Xu *et al.* 2014; Benton *et al.* 2019). The Middle to Late Jurassic hot spring deposits of the Deseado Massif (Patagonia, Argentina) are the only Mesozoic hot spring deposits having been studied in detail (Guido *et al.* 2010; Guido & Campbell 2011; Des Marais & Walter 2019), from which silicified plants, animals, and microorganisms have been documented (Massini *et al.* 2016). Although no feathers have been reported from these hot spring deposits, at the time the deposits were formed, Argentina had diverse dinosaurs (Rauhut *et al.* 2015; Rauhut & Pol 2019). Discoveries of feather-like structures in ornithischian dinosaurs suggest that feathers may have been present in the earliest dinosaurs (Godefroit *et al.* 2014; Xu *et al.* 2014). It seems worthwhile to increase efforts in exploring these hot spring

https://doi.org/10.1017/S1755691022000068 Published online by Cambridge University Press

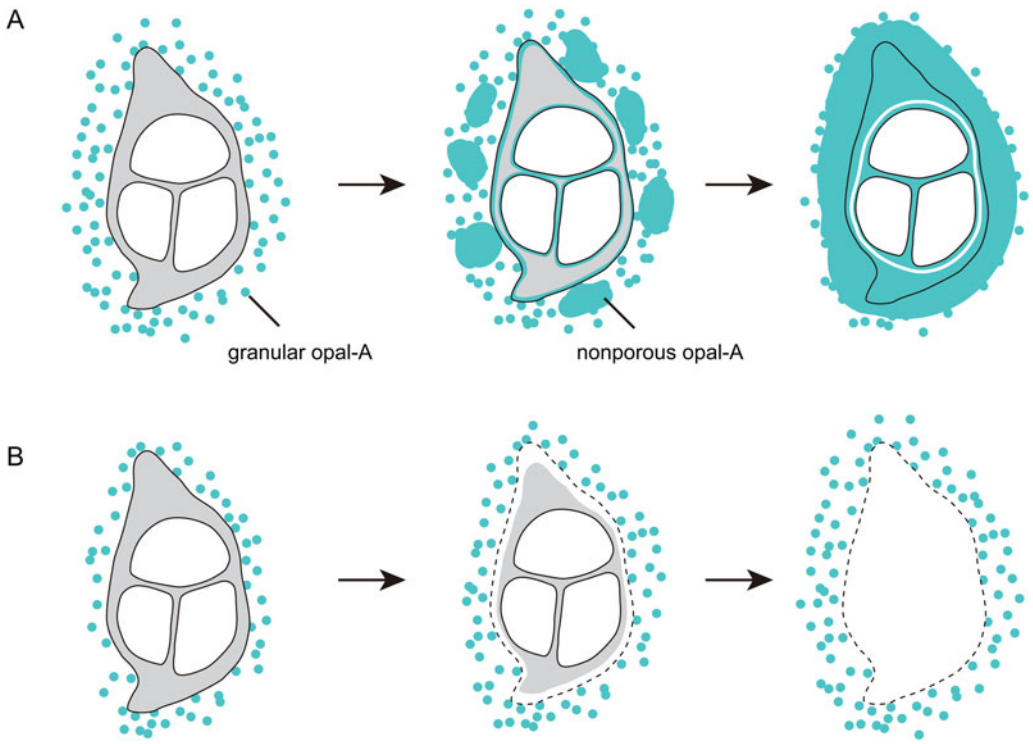

Figure 6 Schematic diagrams of the silicification of feathers. (A) A feather is silicified when the supply of silica is sufficient. (B) A feather is not silicified when the supply of silica is reduced.

deposits for feathers or feather-like structures in order to understand the evolution of feathers and dinosaurs (and see Channing & Edwards 2013, table 2). In comparison, Cenozoic siliceous hot spring deposits (Channing & Edwards 2013, table 1) are more common and usually subject to less diagenetic alterations because of their younger ages (Guidry & Chafetz 2003; Hinman & Walter 2005; Campbell *et al*. 2019), which means that more feathers in better preservation states may be discovered in Cenozoic hot spring deposits.

4. Conclusions

Our results show for the first time that internal silicification of feathers at the cellular level is possible in hot spring vent pools, the water of which is over-saturated with respect to amorphous silica. The SEM-EDS elemental mapping shows that the feathers collected from Champagne Pool are internally silicified to varying degrees and one of them is pervasively silicified. In this highly silicified example, the silicon and oxygen are pervasive in the barb cortex, the membranes of the medullary cells, and barbules, where the abundance of carbon is reduced. By integrating the results from less silicified samples, we establish a sequential process of silicification illustrated graphically in Figure 6.

5. Acknowledgements

We are grateful to Jingjing Tang for photographing the samples and Yan Fang for assistance during SEM observations. The research was supported by the National Natural Science Foundation of China (grant numbers 41902013, 41872016, 41922011, 41688103) and the Strategic Priority Research Program of Chinese Academy of Sciences (grant number XDB26000000).

6. References

Alibardi, L. 2013. Immunolocalization of alpha-keratins and feather beta-proteins in feather cells and comparison with the general process of cornification in the skin of mammals. *Annals of Anatomy* **195**, 189–98.

Alibardi, L. 2017. Review: cornification, morphogenesis and evolution of feathers. *Protoplasma* **254**, 1259–81.

Alleon, J., Bernard, S., Le Guillou, C., Daval, D., Skouri-Panet, F., Pont, S., Delbes, L. & Robert, F. 2016. Early entombment within silica minimizes the molecular degradation of microorganisms during advanced diagenesis. *Chemical Geology* **437**, 98–108.

Benton, M. J., Dhouailly, D., Jiang, B. & McNamara, M. 2019. The early origin of feathers. *Trends in Ecology & Evolution* **34**, 856–69.

Cady, S. L. & Farmer, J. D. 1996. Fossilization processes in siliceous thermal springs: trends in preservation along thermal gradients. *In* Bock, R. B. & Goode, J. A. (eds) *Evolution of hydrothermal ecosystems on earth (and Mars?)*, 150–73. Chichester: John Wiley & Sons.

Campbell, K. A., Guido, D. M., Gautret, P., Foucher, F., Ramboz, C. & Westall, F. 2015. Geyserite in hot-spring siliceous sinter: window on earth's hottest terrestrial (paleo)environment and its extreme life. *Earth-Science Reviews* **148**, 44–64.

Campbell, K. A., Guido, D. M., John, D. A., Vikre, P. G., Rhys, D. & Hamilton, A. 2019. The Miocene Atastra Creek sinter (Bodie Hills volcanic field, California and Nevada): 4D evolution of a geomorphically intact siliceous hot spring deposit. *Journal of Volcanology and Geothermal Research* **370**, 65–81.

Channing, A. & Edwards, D. 2004. Experimental taphonomy: silicification of plants in Yellowstone hot-spring environments. *Earth and Environmental Science Transactions of The Royal Society of Edinburgh* **94**, 503–21.

Channing, A. & Edwards, D. 2009. Silicification of higher plants in geothermally influenced wetlands: Yellowstone as a Lower Devonian Rhynie analog. *PALAIOS* **24**, 505–21.

Channing, A. & Edwards, D. 2013. Wetland megabias: ecological and ecophysiological filtering dominates the fossil record of hot spring floras. *Palaeontology* **56**, 523–56.

Channing, A., Schweitzer, M. H., Horner, J. R. & McEneaney, T. 2005. A silicified bird from quaternary hot spring deposits. *Proceedings of the Royal Society B: Biological Sciences* **272**, 905–11.

Davis, P. G. & Briggs, D. E. 1995. Fossilization of feathers. *Geology* **23**, 783–86.

Des Marais, D. J. & Walter, M. R. 2019. Terrestrial hot spring systems: Introduction. *Astrobiology* **19**, 1419–32.

Dunlop, J. A. & Garwood, R. J. 2018. Terrestrial invertebrates in the Rhynie chert ecosystem. *Philosophical Transactions of the Royal Society B: Biological Sciences* **373**, 20160493.

Feo, T. J., Field, D. J. & Prum, R. O. 2015. Barb geometry of asymmetrical feathers reveals a transitional morphology in the evolution of

https://doi.org/10.1017/S1755691022000068 Published online by Cambridge University Press

avian flight. *Proceedings of the Royal Society B: Biological Sciences* **282**, 20142864.
Foth, C., Tischlinger, H. & Rauhut, O. W. M. 2014. New specimen of *Archaeopteryx* provides insights into the evolution of pennaceous feathers. *Nature* **511**, 79–82.
Garwood, R. J., Oliver, H. & Spencer, A. R. T. 2020. An introduction to the Rhynie chert. *Geological Magazine* **157**, 47–64.
Godefroit, P., Sinitsa, S. M., Dhouailly, D., Bolotsky, Y. L., Sizov, A. V., McNamara, M. E., Benton, M. J. & Spagna, P. 2014. A Jurassic ornithischian dinosaur from Siberia with both feathers and scales. *Science (New York, N.Y.)* **345**, 451–55.
Guido, D. M. & Campbell, K. A. 2011. Jurassic hot spring deposits of the Deseado Massif (Patagonia, Argentina): characteristics and controls on regional distribution. *Journal of Volcanology and Geothermal Research* **203**, 35–47.
Guido, D. M., Channing, A., Campbell, K. A. & Zamuner, A. 2010. Jurassic geothermal landscapes and fossil ecosystems at San Agustín, Patagonia, Argentina. *Journal of the Geological Society* **167**, 11–20.
Guidry, S. A. & Chafetz, H. S. 2003. Anatomy of siliceous hot springs: examples from Yellowstone National Park, Wyoming, USA. *Sedimentary Geology* **157**, 71–106.
Hetherington, A. J. & Dolan, L. 2018. Stepwise and independent origins of roots among land plants. *Nature* **561**, 235–38.
Hinman, N. W. & Walter, M. R. 2005. Textural preservation in siliceous hot spring deposits during early diagenesis: examples from Yellowstone National Park and Nevada, U.S.A. *Journal of Sedimentary Research* **75**, 200–15.
Ji, Q. & Ji, S. 1996. On the discovery of the earliest fossil bird in China (*Sinosauropteryx* gen. nov.) and the origin of birds. *Chinese Geology* **233**, 30–33.
Jones, B. & Renaut, R. W. 2003. Hot spring and geyser sinters: the integrated product of precipitation, replacement, and deposition. *Canadian Journal of Earth Sciences* **40**, 1549–69.
Jones, B., Renaut, R. W. & Rosen, M. R. 1999a. Actively growing siliceous oncoids in the Waiotapu geothermal area, North Island, New Zealand. *Journal of the Geological Society* **156**, 89–103.
Jones, B., Renaut, R. W. & Rosen, M. R. 1999b. Role of fungi in the formation of siliceous coated grains, Waiotapu geothermal area, North Island, New Zealand. *PALAIOS* **14**, 475–92.
Jones, B., Renaut, R. W. & Rosen, M. R. 2001. Taphonomy of silicified filamentous microbes in modern geothermal sinters – implications for identification. *PALAIOS* **16**, 580–92.
Jones, B., Renaut, R. W. & Rosen, M. R. 2003. Taxonomic fidelity of silicified filamentous microbes from hot-spring systems in the Taupo Volcanic Zone, North Island, New Zealand. *Transactions of the Royal Society of Edinburgh: Earth Sciences* **94**, 475–83.
Kamarudin, N. B., Sharma, S., Gupta, A., Kee, C. G., Chik, S. M. S. B. T. & Gupta, R. 2017. Statistical investigation of extraction parameters of keratin from chicken feather using Design-Expert. *3 Biotech* **7**, 127.
Kulp, F. B., D'Alba, L., Shawkey, M. D. & Clarke, J. A. 2018. Keratin nanofiber distribution and feather microstructure in penguins. *The Auk* **135**, 777–87.
Longrich, N. R., Vinther, J., Meng, Q., Li, Q. & Russell, A. P. 2012. Primitive wing feather arrangement in *Archaeopteryx lithographica* and *Anchiornis huxleyi*. *Current Biology* **22**, 2262–67.
Massini, J. G., Escapa, I. H., Guido, D. M. & Channing, A. 2016. First glimpse of the silicified hot spring biota from a new Jurassic chert deposit in the Deseado Massif, Patagonia, Argentina. *Ameghiniana* **53**, 205–30.
McKellar, R. C., Chatterton, B. D. E., Wolfe, A. P. & Currie, P. J. 2011. A diverse assemblage of Late Cretaceous dinosaur and bird feathers from Canadian amber. *Science (New York, N.Y.)* **333**, 1619–22.
Mountain, B. W., Benning, L. G. & Boerema, J. A. 2003. Experimental studies on New Zealand hot spring sinters: rates of growth and textural development. *Canadian Journal of Earth Sciences* **40**, 1643–67.
Orange, F., Lalonde, S. V. & Konhauser, K. O. 2013. Experimental simulation of evaporation-driven silica sinter formation and microbial silicification in hot spring systems. *Astrobiology* **13**, 163–76.
Pan, Y., Zheng, W., Sawyer, R. H., Pennington, M. W., Zheng, X., Wang, X., Wang, M., Hu, L., O'Connor, J., Zhao, T., Li, Z., Schroeter, E. R., Wu, F., Xu, X., Zhou, Z. & Schweitzer, M. H. 2019. The molecular evolution of feathers with direct evidence from fossils. *Proceedings of the National Academy of Sciences* **116**, 3018–23.
Perrichot, V., Marion, L., Néraudeau, D., Vullo, R. & Tafforeau, P. 2008. The early evolution of feathers: fossil evidence from cretaceous amber of France. *Proceedings of the Royal Society B: Biological Sciences* **275**, 1197–202.
Pope, J. & Brown, K. L. 2014. Geochemistry of discharge at Waiotapu geothermal area, New Zealand – trace elements and temporal changes. *Geothermics* **51**, 253–69.
Pope, J. G., McConchie, D. M., Clark, M. D. & Brown, K. L. 2004. Diurnal variations in the chemistry of geothermal fluids after discharge, Champagne Pool, Waiotapu, New Zealand. *Chemical Geology* **203**, 253–72.
Rauhut, O. W. M., Carballido, J. L. & Pol, D. 2015. A diplodocid sauropod dinosaur from the Late Jurassic Cañadón Calcáreo Formation of Chubut, Argentina. *Journal of Vertebrate Paleontology* **35**, e982798.
Rauhut, O. W. M. & Pol, D. 2019. Probable basal allosauroid from the early Middle Jurassic Cañadón Asfalto Formation of Argentina highlights phylogenetic uncertainty in tetanuran theropod dinosaurs. *Scientific Reports* **9**, 18826.
Schweitzer, M. H. 2011. Soft tissue preservation in terrestrial Mesozoic vertebrates. *Annual Review of Earth and Planetary Sciences* **39**, 187–216.
Schweitzer, M. H., Zheng, W., Moyer, A. E., Sjövall, P. & Lindgren, J. 2018. Preservation potential of keratin in deep time. *PLoS ONE* **13**, e0206569.
Toporski, J. K. W., Steele, A., Westall, F., Thomas-Keprta, K. L. & McKay, D. S. 2002. The simulated silicification of bacteria – new clues to the modes and timing of bacterial preservation and implications for the search for extraterrestrial microfossils. *Astrobiology* **2**, 1–26.
Wetmore, A. 1943. The occurrence of feather impressions in the Miocene deposits of Maryland. *The Auk* **60**, 440–1.
Xing, L., Cockx, P. & McKellar, R. C. 2020. Disassociated feathers in Burmese amber shed new light on mid-cretaceous dinosaurs and avifauna. *Gondwana Research* **82**, 241–53.
Xu, X. & Guo, Y. 2009. The origin and early evolution of feathers: insights from recent paleontological and neontological data. *Vertebrata PalAsiatica* **47**, 19.
Xu, X., Zhou, Z., Dudley, R., Mackem, S., Chuong, C.-M., Erickson, G. M. & Varricchio, D. J. 2014. An integrative approach to understanding bird origins. *Science (New York, N.Y.)* **346**, 1253293.
Yang, S., Xu, Y. & Zhang, D. 2006. Morphological basis for the waterproof characteristic of bird plumage. *Journal of Forestry Research* **17**, 163–66.
Zhang, F., Zhou, Z. & Dyke, G. 2006. Feathers and 'feather-like' integumentary structures in Liaoning birds and dinosaurs. *Geological Journal* **41**, 395–404.
Zheng, X., Zhou, Z., Wang, X., Zhang, F., Zhang, X., Wang, Y., Wei, G., Wang, S. & Xu, X. 2013. Hind wings in basal birds and the evolution of leg feathers. *Science (New York, N.Y.)* **339**, 1309–12.

MS received 19 November 2020. Accepted for publication 29 March 2022. First published online 22 April 2022